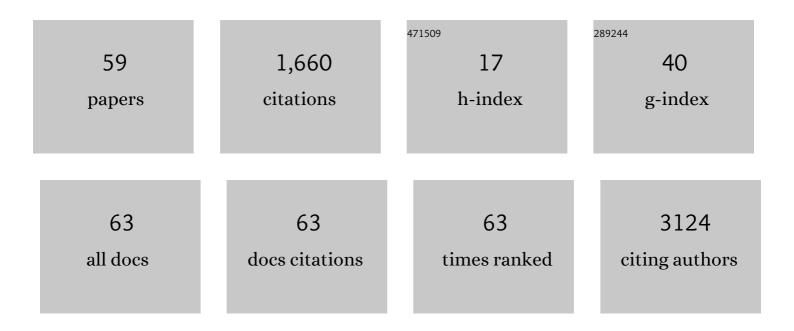
Leonardo Lari

List of Publications by Year in descending order

Source: https://exaly.com/author-pdf/3087777/publications.pdf Version: 2024-02-01



#	Article	IF	CITATIONS
1	Structural evolution of carbon dots during low temperature pyrolysis. Nanoscale, 2022, 14, 910-918.	5.6	21
2	Long-term solar water and CO2 splitting with photoelectrochemical BiOI–BiVO4 tandems. Nature Materials, 2022, 21, 864-868.	27.5	41
3	Linear, tripodal, macrocyclic: Ligand geometry and ORR activity of supported Pd(II) complexes. Inorganica Chimica Acta, 2021, 518, 120250.	2.4	5
4	Optimizing the Electronic Structure of In ₂ O ₃ through Mg Doping for NiO/In ₂ O ₃ p–n Heterojunction Diodes. ACS Applied Materials & Interfaces, 2020, 12, 53446-53453.	8.0	15
5	Optimisation Study of Co Deposition on Chars from MAP of Waste Tyres as Green Electrodes in ORR for Alkaline Fuel Cells. Energies, 2020, 13, 5646.	3.1	13
6	Multi-Walled Carbon Nanotubes Supported Pd(II) Complexes: A Supramolecular Approach towards Single-Ion Oxygen Reduction Reaction Catalysts. Energies, 2020, 13, 5539.	3.1	9
7	In situ TEM oxidation study of Fe thin-film transformation to single-crystal magnetite nanoparticles. Journal of Materials Science, 2020, 55, 12897-12905.	3.7	7
8	Carbon Nitride as a Ligand: Selective Hydrogenation of Terminal Alkenes Using [(Î- ⁵ ₅ Me ₅)IrCl(g ₃ N ₄ â€₽ ² Chemistry - A European Journal, 2020, 26, 6862-6868.	<isNs,Nâ€</i	™₄⁄⊉>)]Cl.
9	Influence of gas environment and heating on atomic structures of platinum nanoparticle catalysts for proton-exchange membrane fuel cells. Nanotechnology, 2019, 30, 175701.	2.6	3
10	Carbon nitride as a ligand: edge-site coordination of ReCl(CO) ₃ -fragments to g-C ₃ N ₄ . Chemical Communications, 2019, 55, 7450-7453.	4.1	10
11	Fractal-like hierarchical organization of bone begins at the nanoscale. Science, 2018, 360, .	12.6	390
12	Monolithic mesoporous graphitic composites as super capacitors: from Starbons to Starenes®. Journal of Materials Chemistry A, 2018, 6, 1119-1127.	10.3	13
13	In-situ Open Cell TEM/STEM Environmental Study of Iron Oxides Nanoparticles and Sample-Beam Interaction in O2 gas. Microscopy and Microanalysis, 2018, 24, 260-261.	0.4	Ο
14	In-situ Visualization and Analysis of Single Atom Dynamics in Chemical Reactions using Novel Environmental-Scanning Transmission Electron Microscopy (ESTEM). Microscopy and Microanalysis, 2018, 24, 1506-1507.	0.4	0
15	Origin of reduced magnetization and domain formation in small magnetite nanoparticles. Scientific Reports, 2017, 7, 45997.	3.3	113
16	Spatially resolved variations in reflectivity across iron oxide thin films. Journal of Magnetism and Magnetic Materials, 2017, 441, 743-749.	2.3	5
17	Polar Spinel-Perovskite Interfaces: an atomistic study of Fe3O4(111)/SrTiO3(111) structure and functionality. Scientific Reports, 2016, 6, 29724.	3.3	10
18	Atomic and electronic structure of twin growth defects in magnetite. Scientific Reports, 2016, 6, 20943.	3.3	15

LEONARDO LARI

#	Article	IF	CITATIONS
19	Recent Progress with AC E(S)TEM and Application to Single Atom Catalysis. Microscopy and Microanalysis, 2015, 21, 731-732.	0.4	0
20	DIY Tomography sample holder. Journal of Physics: Conference Series, 2015, 644, 012013.	0.4	1
21	Control of gas phase nanoparticle shape and its effect on MRI relaxivity. Materials Research Express, 2015, 2, 035002.	1.6	15
22	Sample preparation and EFTEM of Meat Samples for Nanoparticle Analysis in Food. Journal of Physics: Conference Series, 2014, 522, 012057.	0.4	3
23	Correlations between atomic structure and giant magnetoresistance ratio in Co ₂ (Fe,Mn)Si spin valves. Journal Physics D: Applied Physics, 2014, 47, 322003.	2.8	7
24	The Effect of Cobalt-Sublattice Disorder on Spin Polarisation in Co2FexMn1â^'xSi Heusler Alloys. Materials, 2014, 7, 1473-1482.	2.9	9
25	Structural study of Fe ₃ O ₄ (111) thin films with bulk like magnetic and magnetotransport behaviour. Journal of Applied Physics, 2014, 115, 17C107.	2.5	11
26	Tuning Dirac states by strain in the topological insulator Bi2Se3. Nature Physics, 2014, 10, 294-299.	16.7	205
27	Effect of film growth rate and thickness on properties of Ge/GaAs(100) thin films. Thin Solid Films, 2014, 550, 715-722.	1.8	9
28	Enhanced oxidation of nanoparticles through strain-mediated ionic transport. Nature Materials, 2014, 13, 26-30.	27.5	110
29	Over 50% reduction in the formation energy of Co-based Heusler alloy films by two-dimensional crystallisation. Applied Physics Letters, 2014, 105, .	3.3	14
30	Growth of polycrystalline Heusler alloys for spintronic devices. Journal Physics D: Applied Physics, 2014, 47, 265002.	2.8	7
31	Dynamic wet-ETEM observation of Pt/C electrode catalysts in a moisturized cathode atmosphere. Nanotechnology, 2014, 25, 425702.	2.6	15
32	Visualisation of single atom dynamics and their role in nanocatalysts under controlled reaction environments. Chemical Physics Letters, 2014, 592, 355-359.	2.6	46
33	An in-house developed annular bright field detection system. Journal of Physics: Conference Series, 2014, 522, 012016.	0.4	0
34	A STEM study of twin defects in Fe3O4(111)/YZO(111). Journal of Physics: Conference Series, 2014, 522, 012036.	0.4	3
35	Origin of anomalous magnetite properties in crystallographic matched heterostructures: Fe ₃ O ₄ (111)/MgAl ₂ O ₄ (111). Journal of Physics Condensed Matter, 2013, 25, 485004.	1.8	17
36	Fe ₃ O ₄ (1 1 1) thin films with bulk-like properties: growth and atomic characterization. Journal Physics D: Applied Physics, 2013, 46, 022001.	2.8	23

LEONARDO LARI

#	Article	IF	CITATIONS
37	Heusler-alloy films for spintronic devices. Applied Physics A: Materials Science and Processing, 2013, 111, 423-430.	2.3	70
38	Exchange Bias in Fe@Cr Core–Shell Nanoparticles. Nano Letters, 2013, 13, 3334-3339.	9.1	42
39	Magnetism and magnetotransport in symmetry matched spinels: Fe3O4/MgAl2O4. Journal of Applied Physics, 2013, 113, 17B107.	2.5	13
40	GaN-based radial heterostructure nanowires grown by MBE and ALD. Journal of Physics: Conference Series, 2013, 471, 012039.	0.4	1
41	Correlation of Microstructure and Transport Properties of Multilayered Graphene Spin Valves on SiO ₂ /Si. Journal of Physics: Conference Series, 2013, 471, 012048.	0.4	1
42	ESTEM imaging of single atoms under controlled temperature and gas environment conditions in catalyst reaction studies. Annalen Der Physik, 2013, 525, 423-429.	2.4	66
43	Effect of Seed Layers on Polycrystalline \${m Co}_{2}{m FeSi}\$ Thin Films. IEEE Transactions on Magnetics, 2012, 48, 4006-4009.	2.1	4
44	Structural and magnetic properties of epitaxial In1–xMnxSb semiconductor alloys with x > 0.08. Journal of Vacuum Science and Technology B:Nanotechnology and Microelectronics, 2012, 30, 032801.	1.2	5
45	Room-temperature structural ordering of a Heusler compound Fe <mml:math xmlns:mml="http://www.w3.org/1998/Math/MathML" display="inline"><mml:msub><mml:mrow /><mml:mn>3</mml:mn></mml:mrow </mml:msub>Si. Physical Review B, 2012, 86, .</mml:math 	3.2	48
46	Characterization of InMnSb epitaxial films for spintronics. Journal of Physics: Conference Series, 2012, 371, 012032.	0.4	4
47	Structural study of Ge/GaAs thin films. Journal of Physics: Conference Series, 2012, 371, 012040.	0.4	7
48	Preparation of hydrosol suspensions of elemental and core–shell nanoparticles by co-deposition with water vapour from the gas-phase in ultra-high vacuum conditions. Journal of Nanoparticle Research, 2012, 14, 1.	1.9	33
49	The effect of interfaces on magnetic activation volumes in single crystal Co2FeSi Heusler alloy thin films. Applied Physics Letters, 2012, 101, 102410.	3.3	7
50	Ferromagnetic InMnSb multi-phase films study by aberration-corrected (scanning) transmission electron microscopy. Journal of Applied Physics, 2012, 111, 07C311.	2.5	32
51	Accurate calibration for the quantification of the Al content in AlGaN epitaxial layers by energy-dispersive X-ray spectroscopy in a Transmission Electron Microscope. Journal of Physics: Conference Series, 2011, 326, 012028.	0.4	3
52	Comparison of the contrast in conventional and lattice resolved ADF STEM images of InGaAs/GaAs structures using different camera lengths. Journal of Physics: Conference Series, 2011, 326, 012041.	0.4	4
53	Properties of GaN Nanowires Grown by Molecular Beam Epitaxy. IEEE Journal of Selected Topics in Quantum Electronics, 2011, 17, 878-888.	2.9	104
54	Direct observation by transmission electron microscopy of the influence of Ni catalyst-seeds on the growth of GaN–AlGaN axial heterostructure nanowires. Journal of Crystal Growth, 2011, 327, 27-34.	1.5	4

LEONARDO LARI

#	Article	IF	CITATIONS
55	GaN, AlGaN, HfO ₂ based radial heterostructure nanowires. Journal of Physics: Conference Series, 2010, 209, 012011.	0.4	6
56	Electron microscopy of AlGaN-based multilayers for UV laser devices. Journal of Physics: Conference Series, 2010, 241, 012048.	0.4	0
57	Defect characterization and analysis of Illâ€V nanowires grown by Niâ€promoted MBE. Physica Status Solidi (A) Applications and Materials Science, 2008, 205, 2589-2592.	1.8	7
58	Nanoscale compositional analysis of Ni-based seed crystallites associated with GaN nanowire growth. Physica E: Low-Dimensional Systems and Nanostructures, 2008, 40, 2457-2461.	2.7	20
59	Quantitative EELS Analysis of AlGaN Nanowires Grown by Ni Promoted MBE on Sapphire Substrate. Materials Research Society Symposia Proceedings, 2007, 1026, 1.	0.1	2